PREPRINT of the paper published in:
***Energy & Fuels*, V.24, Iss.7, pp.3959-3969 (2010).**

Electrical Conductivity and Dielectric Properties of Solid Asphaltenes

Igor N. Evdokimov,* and Aleksandr P. Losev

Department of Physics, Gubkin Russian State University of Oil and Gas, Leninsky Prospekt, 65, Moscow B-296, GSP-1, 119991, Russia

Abstract

DC and AC (120 and 1000 Hz) conductivity and AC dielectric properties of solid precipitated asphaltenes have been studied at temperatures 5 - 105 ^{o}C. The temperature dependencies revealed the presence of a structural transition, ascribed to changes in the predominant type of intermolecular bonding. Apparently, at solid surfaces this transition occurs at absolute temperatures about 20 % lower than in the solid bulk. Analysis of conductivity mechanisms is supplemented by comparison of UV-vis-NIR absorption spectra for solid asphaltenes and for their solution in toluene. It is concluded that in solid asphaltenes surface conductivity is always predominant over the bulk one. The major transport mechanism of charge carriers at asphaltene surfaces appears to be unidirectional electron hopping between spatially close shallow localized traps. The dielectric constant of solid asphaltenes below 35 - 40 ^{o}C was found to be both frequency and temperature independent and was evaluated as $\varepsilon = 4.3 \div 5.4$.

---

* To whom correspondence should be addressed. E-mail: physexp@gubkin.ru

Introduction

Asphaltenes remain the most studied and yet least understood materials in the petroleum industry - despite numerous publications on the topic of asphaltene characterization, information on their properties frequently appears to be non-conclusive and misleading.[1] For instance, from the practical point of view, knowledge of electrical and dielectric characteristics of precipitated solid asphaltenes is important for solving deposition problems.[2-4] However, since the pioneering study of Lichaa and Herrera,[5] the term "electrical conductivity of asphaltenes" was misleadingly employed to characterize the movement of charged asphaltene colloids within crude oils and solvents.[6-9] With the exception of ref.3, there have been no publications on electrical conductivity via the transport of charge carriers within solid asphaltenes themselves. Furthermore, all available data on dielectric constant ε (static permittivity) have been obtained in asphaltene solutions of varying concentrations by extrapolating the data to "the solid bulk state" according to various theoretical assumptions.[3,10-16] Not surprisingly, the reported values of ε vary almost by an order of magnitude, as illustrated in Table 1.

Table 1. Extrapolated dielectric constants of solid asphaltenes from earlier experiment with solutions of varying concentrations.

ε	2.44; 2.51	2.48 - 2.71	2.7	3.83	5.0 – 7.0	5.2; 6.8; 7.1	6.16; 6.92	5.5 - 18.4
ref.	(10)	(11)	(12)	(3)	(13)	(14)	(15)	(16)

Previous asphaltene studies have been performed both at direct current (DC) conditions and at various frequencies of alternating current (AC). The basic concepts of the employed theoretical analysis may be summarized as follows.[2,17]

Dependent upon the frequency range, the complex electrical behavior of asphaltenes may result from their dipolar (dielectric) response, their conductive response, or both. The dielectric response is commonly presented as the real and imaginary parts of the complex relative permittivity, ε^*:

$$\varepsilon^* = \varepsilon' - i\varepsilon'' \qquad (1)$$

The real component of ε^* can be found from measurements of capacitance. In case ε' is frequency-independent, it coincides with a static dielectric constant ε. For a parallel-plate capacitor with a space-filling (e.g., liquid-state) sample:

$$\varepsilon' = (C-C_L)d/S\varepsilon_0 \qquad (2)$$

where C is the measured capacitance, C_L is the lead capacitance, d is the gap between metal contacts, S is the contact area, and ε_0 is the permittivity of free space. For solid granular (powder) samples:

$$\varepsilon' = (C-C_L)d/\phi S\varepsilon_0 \qquad (2a)$$

where ϕ is the packing fraction - the total volume of solid matter divided by the total volume of the sample.

The imaginary component of ε^* usually is referred to as dielectric loss (or as loss factor). Most often it is evaluated by measurements of the dielectric loss tangent $tan\delta$:

$$tan\delta = \varepsilon''/\varepsilon' \qquad (3)$$

In a dielectric material, there are both free and bound ions, resulting in conductivity and dipolar contributions to the dielectric loss:

$$\varepsilon'' = \varepsilon''_{cond} + \varepsilon''_{dipol} \qquad (4)$$

with the conductivity contribution normally dominant at low frequencies ν of the applied electric field:

$$\varepsilon''_{cond} = \sigma/(2\pi\nu\varepsilon_0) \qquad (5)$$

where the directly measured conductivity σ is considered to be frequency-independent, the dielectric loss factor is thus proportional to the reciprocal of applied frequency.[2,17]

Asphaltenes may be regarded as condensed polynuclear aromatic compounds[1] which possess a semiconductor-type conductivity.[18,19] Most frequently, temperature dependence of conductivity of pure materials (in the absence of strong disorder or specific structural transformations) is expressed as:

$$\sigma = \sigma_0 exp(-E_a/kT) \qquad (6)$$

where σ_0 is a material constant and E_a, k and T are, respectively, the apparent activation energy for conduction, Boltzmann's constant and the absolute temperature.

Of immediate relevance to conductivity experiments described in this paper are previous studies of microstructural transformations in solid asphaltenes at temperatures below 100 - 150 ^oC. These transformations have been revealed by measurements of thermal properties, mainly by differential scanning calorimetry (DSC).[20-24] Masson et al.[20] concluded that solid asphaltenes lack a crystalline phase, but have an ordered amorphous phase (mesophase) which is identified by an endotherm at around 50 °C in the DSC heat flow curves. They also identified two overlapping glass transitions in the amorphous domains of asphaltenes, the prevalent one at 70 °C apparently controlled by interactions, involving oligo-aromatic structures in asphaltenes. Maham et al.[21] indicated that asphaltenes are in a state of an ordered solid at low temperatures, while a broad endothermic transition arises on heating at -13 ^oC and an exothermic transition begins to dominate around 77 ^oC. The authors concluded that asphaltenes exhibit polymorphism, i.e. that they comprise two phases over a broad range of conditions. In particular, one fraction of the asphaltenes undergoes melting or a glass transition (endotherm) while another fraction dissolves

into it (exotherm) at higher temperature. The endothermic and exothermic processes observed were shown to be reversible, while the low-temperature phase was structurally controlled by interactions between polar alkane side chains in asphaltenes.[21,26] However, these studies showed that asphaltenes exhibit phase transition at lower temperature on cooling than on heating in a systematic manner.[21] Fulem at al.[23] reported a broad endothermic transition from an amorphous solid to liquid commencing at 67 ^{o}C. They also suggested that the presence of the overlapping exotherm was consistent with a fraction of solid asphaltenes dissolving into liquid asphaltenes. Rodriguez-Abreu et al.[22] identified in bulk asphaltenes a broad endothermic peak centered at around 60 ^{o}C. A step-like variation of the DSC curve at around 40 ^{o}C they attributed to the occurrence of a second-order phase transition. Tran[24] observed a broad and reversible endothermic transition in asphaltenes (interpreted as a solid or glass to liquid transformation), beginning at temperatures below 47 ^{o}C. There was also an exothermic transition, beginning at approximately 105 ^{o}C. The author concluded that asphaltenes exhibit a minimum of two phases over the studied temperature interval and that details of the phase behavior and thermophysical properties of asphaltenes are functions of their previous thermal history, in particular of heating above 105 - 110 ^{o}C. DSC heat flow curves of asphaltenic crude oils from various geographic locations also revealed common endothermic minima in temperature ranges of 40 - 45 and 95 - 100 ^{o}C.[25] It may also be noted, that studies of asphaltenes in solutions have indicated a transformation to a more dense asphaltene phase on heating above 35 - 40 ^{o}C.[27,28]

Summarizing, the presence of two phase transformations at ≤100 - 150 ^{o}C and the corresponding two-phase behavior observed by various authors appear to be common properties of asphaltenes from diverse geological/geographical origin. The complexity of thermal curves suggests the occurrence of several molecular processes, probably due to variations of the

microstructure of asphaltenes, which are inhomogeneous systems and contain microdomains differing in structure and composition.[22] On the other hand; thermal effects may correspond to aggregation-dissociation of certain components of the asphaltene. The structure of the low-temperature phase appears to be controlled by interactions between polar side chains of asphaltene molecules, while in the higher-temperature phase, interaction involving flat polyaromatic structures in asphaltenes become more important.

In this paper, we report on the DC and AC conductivity and the AC dielectric properties of precipitated solid asphaltenes. Low AC frequencies (120 Hz and 1000 Hz) were employed, in the range where conduction effects are believed to play a key role. The temperature dependencies were investigated to reveal possible effects of structural transformations in solid asphaltenes. The results are supplemented by comparison of UV-vis-NIR absorption spectra for solid asphaltenes and for their solution in toluene.

Experimental Section

Samples. The solid asphaltenes have been provided by the ‘‘TATNEFT’’ oil production company and used as received. These asphaltenes have been precipitated from a mixture of Tatarstan virgin crude oils (Romashkinskoye reservoir) by the standard technique of dilution with 40 volumes of n-heptane at room temperature. The original asphaltene sample (#1) was in a state of a powder with irregular grains of 10.6 μm median size, and was stored in the dark, in air. To remove possible foreign contaminants, sample #2 was prepared by dissolving original asphaltenes in toluene, filtering the solution and evaporating the excess solvent at 105 ^{o}C. Solid deposits have been hand-ground in pestle and mortar to get powder with grain size close to that of sample #1. Weighted portions of the filtered solution were evaporated inside the test cell to

obtain solid asphaltene films with thicknesses of 50-80 μm. The homogeneity of films was assessed by thickness measurements in various parts of each film. Typical thickness variations were within 3-6%. The continuity of films was assessed by resistivity measurements. Continuous films were highly insulating, with the resistance above 10^7 Ohms even at temperatures as high as 80 ^oC. Loss of continuity as a result of pinhole punctures introduced to the films, decreased resistance at 80 ^oC below 10^3 Ohms. The continuous film sample employed in the below described experiments was obtained by depositing ca. 27 mg of dry asphaltenes and had an average thickness of 52 μm.

Test Cell. The cell was that previously employed for high-frequency dielectric studies of petroleum,[29] and designed for AC measurements at frequencies up to 10 GHz (Figure 1). The cell contained two cylindrical electrodes of 23.90 mm in diameter. Asphaltene powders were hand-compacted (estimated pressures not exceeding 0.1 MPa) inside a teflon guard ring to samples of 0.96 mm in thickness and of 22.40 mm in diameter. For technical reasons, a guard ring could not be employed in course of asphaltene film preparation. Consequently, an area of the film sample was somewhat larger than the area of electrodes which precluded evaluation of a dielectric constant in this case. The test cell was temperature controlled with 0.1 ^oC accuracy in the range of 5 - 105 ^oC.

Apparatus. DC conductivity (in kOm^{-1} units) was determined using AKTAKOM ABM-4307 meter from current-voltage dependencies in the ranges of 0 - 10 V and of 0 - 100 V. AC resistance R, capacitance C and loss tangent $tan\delta$ were measured using an AKTAKOM AM-3002 LCR meter, at two frequencies of 120 Hz and of 1000 Hz, with a 0.9 V applied voltage. AC conductivity was evaluated as $\sigma = 1/R$ (in kOm^{-1} units); according to Eq. (2) and Eq. (3), dielectric loss was evaluated as $\varepsilon'' = tan\delta \cdot \varepsilon' = B \cdot C \cdot tan\delta$, where a constant B was adjusted

assuming proportionality of ε'' and σ specified in Eq.(5). The optical absorption spectra in the range from near-UV to near-IR (312 – 995 nm) have been studied using a spectrometer, routinely employed in Russian oilfield laboratories, namely, a KFK-3 Photocolorimeter.

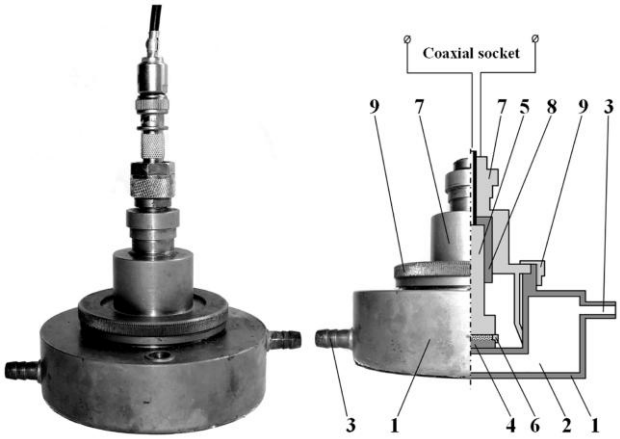

Figure 1. The test cell. 1. - cell body; 2 - thermal fluid chamber; 3 - connection nipples to circulating thermostat; 4 - bottom cylindrical electrode; 5 - upper cylindrical electrode; 6 - teflon guard ring; 7 – upper electrode holder; 8 - teflon insulator; 9 – hold-down nut.

Results and Discussion

Ohmic Character and Frequency Independence of Conductivity. In all studied cases the DC conductivity σ_{dc} of asphaltene samples was ohmic in the voltage ranges employed, as illustrated in Figure 2A. At the low frequencies of 120 Hz and 1000 Hz employed in these studies, the measured AC conductivities σ_{120} and σ_{1000} of all samples appeared to be frequency independent and (within random variations of ca. ± 2%) equal to σ_{dc} in the entire range of studied temperatures (cf. Figure 2B). It should be noted that in the film state, asphaltene sample #2 was highly insulating at lower temperatures, so its conductivity could be reliably detected only above 60 - 70 ^{o}C.

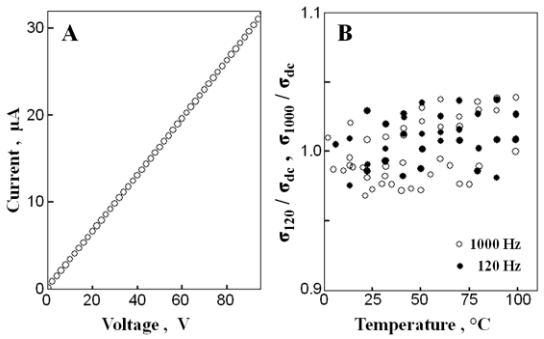

Figure 2. A - ohmic behavior of DC conductivity (sample #2, powder; at 25 ^{o}C); **B** – frequency independence of AC conductivity (sample #1, powder; sample #2, powder; sample #2, film).

Effects of Temperature on Conductivity. For each sample, initial experiments were performed at room temperature (22 - 24 ^{o}C). These were followed by thermal treatment in several heating/cooling cycles in the temperature range of 5 - 105 ^{o}C. Each temperature experiment was conducted at ambient atmosphere according to the same standard procedure. Namely, a typical heating/cooling rate was 0.5 ^{o}C/min, i.e. in cycles with 5 ^{o}C temperature increments, ca. 10 minutes was allowed for stabilization of the temperature and sample properties before each measurement; accordingly, for 10 ^{o}C increments the stabilization time was twice longer. A typical time interval between successive heating/cooling cycles was 14 - 16 hours, apparently sufficient for the complete restoration of the below discussed low-temperature states of the samples.

For convenience of further discussion, the observed temperature effects may be subdivided into short-, intermediate- and long-term ones. The most representative of short-term effects (on the time sale of minutes) is a reproducible manner of conductivity increase on heating, exhibiting sensitivity to phase transformation in the microstructure (molecular arrangement) of asphaltene samples (cf. further discussion of Figures 5, 6 and 7). An intermediate-term effect is a noticeable thermal hysteresis of heating/cooling cycles in asphaltene powders, as illustrated in

Figure 3 for conductivity, normalized to its value at 5 ^{o}C. As augmented in more detail below, this hysteresis we ascribe mainly to the lower-temperature "surface" phase transition in asphaltenes (irreversible on the short-time scale). Figure 3 shows also a virtual absence of hysteresis in an asphaltene film, where a predominant phase transition is a higher-temperature "bulk" one.

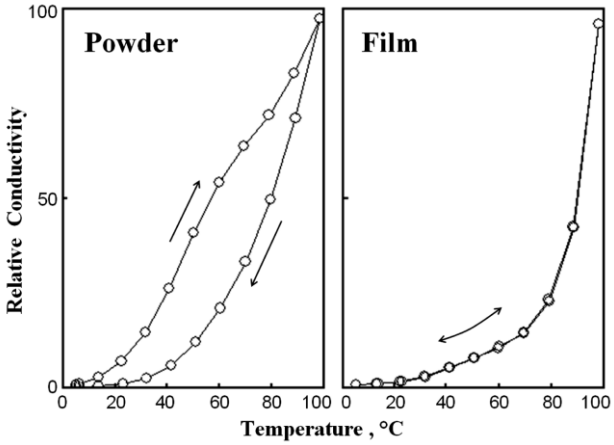

Figure 3. Thermal hysteresis of a heating/cooling cycle in asphaltene powder and its apparent absence in an asphaltene film (sample #2, measurements at 1000 Hz)

Finally, the long-term effects (on the time scale of days) are non-reversible conductivity variations in course of prolonged thermal treatment in successive heating/cooling cycles, as illustrated in Figure 4. Visual examination of treated samples revealed corresponding noticeable changes in their macrostructure. Namely, a decrease of σ in asphaltene powders was accompanied by a decrease of the open surface area (increase of homogeneity) via sintering of original grains. On the other hand, an increase of conductivity in asphaltene film was accompanied by a growth of open surfaces (loss of homogeneity) via appearance of multiple breaks, cracks and punctures, as illustrated at the inset of Figure 4B. Taking into account a negligible conductivity of the non-heated film, we may conclude that in solid asphaltenes the

predominant transport mechanism of charge carriers is not through the bulk but along the open surfaces of macrostructural defects /inhomogeneities. The predominance of surface (grain boundary) conductivity is a common property of porous/grainy materials, where a decrease of surface area in sintered samples was observed to decrease the measured σ values.[30,31]

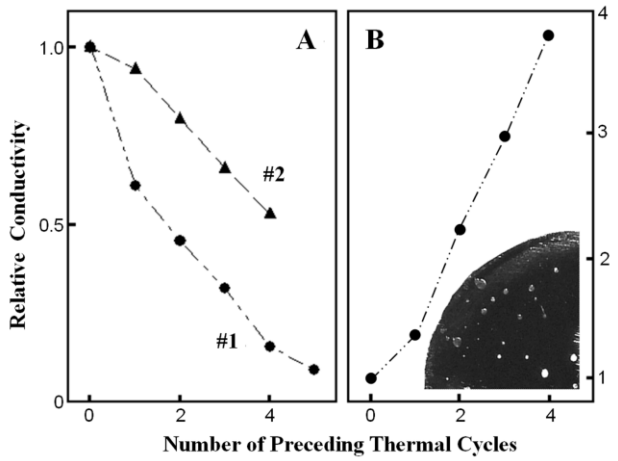

Figure 4. Non-reversible conductivity variations in course of prolonged thermal treatment. **A** – powder samples #1 and #2; measurements at 22 ^{o}C. **B** – film sample #2; measurements at 70 ^{o}C. The inset shows a photograph of the asphaltene film with multiple punctures appeared after five thermal cycles.

Sensitivity of Conductivity and Dielectric Loss to Structural Transformations in Asphaltenes. As noted above, in spite of non-reversible variations of the absolute values of conductivity, the measured $\sigma(T)$ dependencies appeared to be similar in shape. In particular, for powder samples, a striking coincidence of the derivatives $d\sigma/dT$ was observed in all heating experiments – cf. open circles in Figure 5A. Moreover, in spite of the below discussed deviations from the expected proportionality between conductivity σ and dielectric loss ε'' (cf. Eq. (5)), the behavior of derivatives $d\varepsilon''/dT$ (filled circles in Figure 5A) was similar to that of $d\sigma/dT$. Both derivatives exhibit a well-defined broad maximum, centered at ca. 40 ^{o}C. Figure 5B shows that

this is fairly close to positions of broad endothermic peaks, observed by DSC studies of solid asphaltenes in ref.(20) (curve1) and ref.(22) (curve 2). A second increase of derivatives in Figure 5A commences at 70 - 80 ^{o}C and obviously continues beyond 105 ^{o}C, the upper boundary of the studied temperature range. Taking into account previous publications on thermal properties of solid asphaltenes,[20-24] the observed short-term behavior of $d\sigma/dT$ and of $d\varepsilon''/dT$ on heating may be attributed to phase transitions in asphaltene microstructure. Note, that on short time scales (up to one-two hours) the lower temperature transition appears to be irreversible, as illustrated in Figure 5A by a smooth behavior of $d\sigma/dT$ for a cooling branch of the thermal cycle (sample #2, powder).

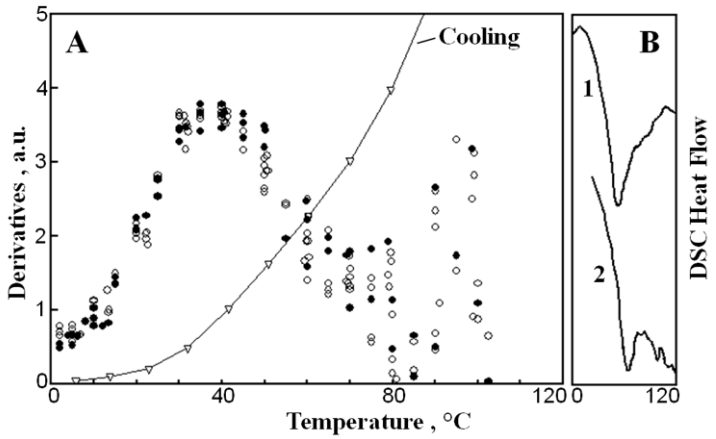

Figure 5. A. – In powder samples, derivatives of conductivity (open circles) and of dielectric loss (filled circles) reveal structural transformations in solid asphaltenes on heating; on subsequent cooling the observed behavior of derivatives is featureless (triangles), indicating irreversibility of the lower-T transformation on short time scales. **B.** – Earlier evidence of the observed phase transformations provided by DSC studies of solid asphaltenes.

In contrast to the data for powder samples, in heating experiments with an as-deposited asphaltene film sample, the derivatives $d\sigma/dT$ and of $d\varepsilon'/dT$ did not show any evidence of a phase transition close to 40 ^{o}C (cf. Figure 6). Only in a thermally aged film, with multiple visible

punctures, a very weak maximum started to appear in this temperature range. On the other hand, like in powder samples, a sharp increase of derivatives above 70 - 80 ^{o}C was observed in all experiments with an asphaltene film. A plausible explanation for the differences/similarities of the powder and film states may be that only the structural transformation commencing at 70 - 80 ^{o}C and extending above 105 ^{o}C is a true "bulk" (3D) one. The lower-temperature transition at around 40 ^{o}C apparently reflects some structural transformation at the open boundaries of powder grains and of film defects and most probably may be classified as a "surface" (2D) transition. As a rule, surface transitions are genetically coupled to a bulk one at higher temperatures, i.e. are governed by the same underlying molecular mechanisms (cf. also discussion of Figure 11). For example, before "bulk melting", distinct stages of ''surface premelting'' and of ''surface melting'' have been observed in some metals.[32] Surface premelting is the initial disordering of surface atoms usually as the result of formation of vacancy/adatom pairs. In contrast, surface melting is the formation, just below the bulk melting point, of a quasi-liquid skin on the surface, whose thickness diverges as the melting point is approached.[32]

Summarizing, our results reported in Figures 5 and 6 suggest that two seemingly unrelated phase transitions temperatures (105 – 110 ^{o}C and 40 – 50 ^{o}C) may reflect molecular processes of the same origin, but in different domains of asphaltene samples – in the bulk and in the interface layer. As follows from prior works on thermal analysis of asphaltenes,[20-25] discussed in Introduction, structural transformations in this temperature range may belong t the type of solid to liquid transitions. Hence, they may be directly responsible for the above discussed non-reversible sintering in asphaltene powders and loss of homogeneity in asphaltene films (cf. Figure 4).

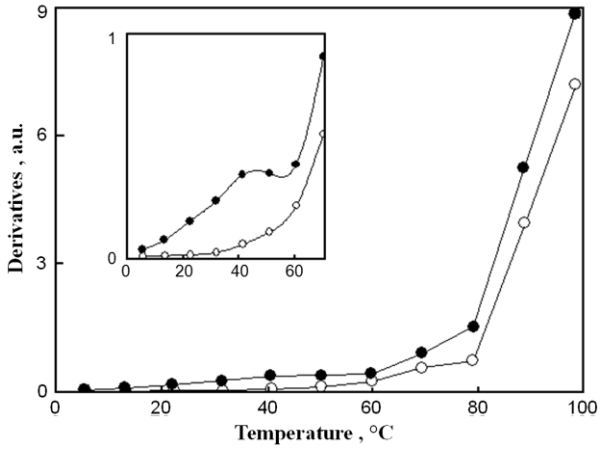

Figure 6. An apparent absence of low-temperature structural transformation in a homogeneous asphaltene film. Open circles - as-deposited film; filled circles – thermally aged (punctured) film. Low-temperature parts of the curves are magnified in the insert.

Some additional information on characteristics of phase transformations in asphaltenes may be obtained by comparing temperature dependencies of conductivity σ and of dielectric loss ε'', as illustrated in Figure 7. Namely, if dipolar relaxation processes $\varepsilon''_{\text{dipol}}$ are negligible, at any given frequency $\varepsilon'' = \varepsilon''_{\text{cond}}$ and should be directly proportional to σ (cf. Eq. 4 and Eq. 5), hence the ratio ε''/σ may be expected to remain constant and temperature-independent. Figure 7 shows that such behavior was observed in various thermal cycles only for the above discussed low-temperature asphaltene phase, while after the phase transition at 35 - 40 ^{o}C the loss-to-conductivity ratio reproducibly increased (by ca. 4%), indicating an emerging significance of $\varepsilon''_{\text{dipol}}$. A plausible explanation is that in a low temperature phase, cross-linking by asphaltene side chains arrests the motion of polar moieties present in asphaltenes (e.g., pyridinic and pyrollic nitrogen, phenolic hydroxyl, carboxylic groups, and quinonic oxygen[33]). After the phase transformation, these polar groups may be liberated as the structure-defining interaction becomes π-bonding among aromatic moieties.

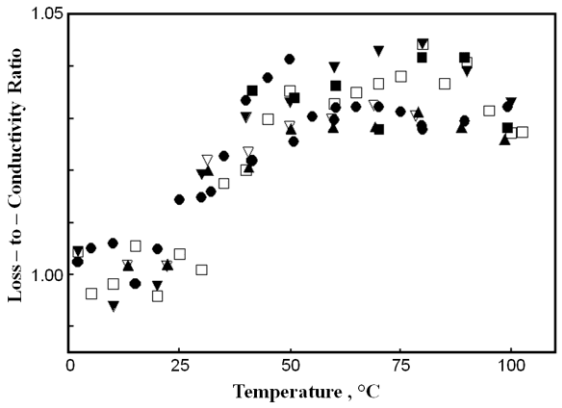

Figure 7. Effects of structural transformation in asphaltenes on the ratio ε''/σ in powder samples #1 and #2 (measurements at 1000 Hz).

Possible Conductivity Mechanisms in Solid Asphaltenes. As concluded above, the predominant transport mechanism of charge carriers in studied samples is a surface-controlled one, typical for insulating materials and organic semiconductors, while in conventional semiconductors σ measurements usually are relatively insensitive to surface processes due to conducting paths through the bulk.[34] It is well known that surface mechanisms of conductivity in porous materials (e.g., powders, ceramics, coatings) may be strongly affected by adsorption of water and oxygen from ambient atmosphere.[31,34-38] E.g.. conductivity variations of ceramic powders in ref.31 were explained by removal of 0.7 monolayers of physisorbed water, as evidenced by 0.40 % weight loss in samples heated from 30 to 100 ^{o}C. Gravimetric measurements of our powder asphaltene samples also revealed a weight loss of 0.35 % on heating from 20 to 90 ^{o}C, which (taking into account some differences in the size of powder grains) may be indicative of removal of ca. one monolayer of adsorbed water. However, it should be emphasized that in case of the determining role of surface adsorption, adsorbed species always increase conductivity. Hence, a common effect of thermal treatment of such materials is a noticeable decrease of conductivity in course of heating due to removal of absorbed water[31,34,36]

or oxygen.[37,38] On the contrary, in all our experiments, heating of asphaltene samples always was accompanied by an increase of conductivity (cf. Figure 3) indicating a negligible role of absorbed (extrinsic) charge carriers.

Furthermore, we conclude that intrinsic ionic conductivity is also negligible in our case for the following reasons. Firstly, as noted above, the measured σ values were frequency-independent, while ionic conductivity (via translational motion of charge carriers) is known to vary noticeably even in the low-frequency range.[30,31,36] Secondly, typical activation energies E_a of ionic conductivity, as determined by Eq. (6), commonly are 1 eV and above, both for bulk and grain boundary processes,[30,31] i.e. much higher than below evaluated E_a values for our asphaltene samples. Finally, as discussed below, there is a definite relation of the measured E_a to the optical energy gap in asphaltenes, a feature that can not be expected in case of ionic conductivity.

Summarizing, the major conductivity mechanism in studied asphaltene samples appears to be that of electron conduction. For intrinsic electronic conduction in organic/molecular solids, the most important parameters are the so-called "energy gaps" E_g, separating the highest occupied energy levels from the lowest unoccupied accessible levels.[39,40] Independent evaluation of E_g may be achieved by measuring optical absorption spectra and analyzing experimental data in the framework of the Tauc model:[41]

$$\alpha \cdot h\nu = B \cdot (h\nu - E_g)^2 \qquad (7)$$

where α is the absorption coefficient and $h\nu$ is the photon energy. The B factor has been frequently taken as a measure of the structural disorder in the material, in the sense that a higher value for B would indicate a lower degree of structural disorder.[41]

In practice, the values of E_g are obtained by plotting the Tauc parameter $(\alpha \cdot h\nu)^{1/2}$ as a function of $h\nu$ and extrapolating the linear parts of the plot to the photon energy axis. The slope of the straight line is $B^{1/2}$.

We have performed optical absorbance measurements at room temperature (22 ^{o}C) for a solid film of sample #2 asphaltenes and for a solution of these asphaltenes in toluene. The measured spectra are presented in Figure 8A. The insert shows a characteristic absorption band at ca. 920 nm (E_b = 1.34 eV), observed only for solid asphaltenes and absent in the spectra of asphaltene solution. The respective Tauc plots in Figure 8B show that the higher-energy gap for solid asphaltenes E_{g1} = 1.86 eV is noticeably smaller than that for colloidal asphaltenes dispersed in solvent (2.01 eV), while the lower-energy gaps are similar (E_{g2} = 0.91 eV). As may have been expected, increased order in the solid state was accompanied by a strong increase in the values of the respective B factors.

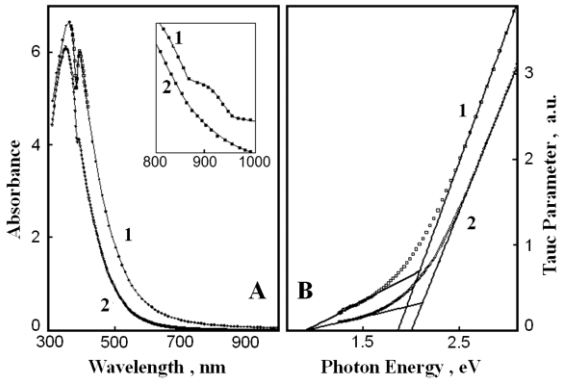

Figure 8. Evaluation of electron energy bands from optical adsorption spectra of a solid asphaltene film (1) and of a toluene solution of asphaltenes (2). **A** – a conventional plot of the measured spectra. **B** – a Tauc plot for determination of energy gaps.

In case of asphaltene conductivity arising solely from interband electron transitions, the activation energies in Eq. (6) may be expected to be equal to $E_g/2$,[39] (i.e. the highest activation energy in our case should be $E_a = E_{g1}/2$ = 0.93 eV). Indeed, intrinsic conductivity with $E_a = E_{g1}/2$

was observed in a family of purified condensed polynuclear aromatic compounds with 6-12 aromatic rings[42] and in other aromatic hydrocarbons.[43] The electronic conductivity of these substances in the solid crystalline state has been attributed to π- electrons of the conjugated aromatic systems, while the values of E_{g1} and E_a were found to be closely correlated to the numbers of aromatic rings, and not affected greatly by the particular shapes of molecules.[42] If this correlation is extended to asphaltenes, the above E_{g1} value of 1.86 eV would indicate the presence of no more than 4 - 5 condensed rings in their aromatic systems.

It has been observed that in the presence of impurities (as expected in petroleum-derived asphaltenes) and macrostrucrural defects (e.g. in powder samples) the measured activation energies of electron conductivity may fall below the upper limit of $E_{g1}/2$.[42,43] Furthermore, enhanced disorder coming from impurities or structural defects in non-single-crystal materials (e.g., microcrystalline, amorphous, glassy) usually sets limits on applicability of the simple Arrhenius-type temperature dependence of conductivity with an activation energy E_a as a principle parameter. Strictly, Eq. (6) describes free carrier conduction with single-type thermal excitation of electrons to a well-defined energy band or an extended impurity state. In disordered systems with conduction via hopping of charge carriers between neighboring localized states, Eq. (6) is frequently supplemented by application of the below discussed Meyer–Neldel rule. A more fundamental revision is a model of conductivity, considering also electron hopping between localized states which may not be nearest neighbors, but may be of variable distance away, i.e. "variable range hopping" (VRH) model, developed by Mott and Davis.[44] Temperature dependence of conductivity in the VRH model may be expressed as:[44,45]

$$\sigma = \frac{\sigma_{MD}}{\sqrt{T}} \exp\left[-\left(\frac{T_0}{T}\right)^{\frac{1}{4}}\right] \qquad (8)$$

where the parameter that accounts for effective energy of charge carrier activation is the "characteristic temperature" T_0.

In the assumption of Arrhenius-type conductivity mechanisms, the measured $\sigma(T)$ dependencies are conventionally analyzed by plotting graphs of Ln(σ) vs. 1/T. The values of E_a are then determined from the slopes of straight-line segments of the graphs. In the assumption of VRH-type conductivity, the respective procedure of T_0 evaluation is by plotting graphs of Ln($\sigma T^{1/2}$) vs. $T^{1/4}$. Figure 9 shows both types of such plots for some experimental $\sigma(T)$ dependencies obtained during heating of asphaltene powder samples #1 and #2. A noticeable curvature of both plots is clearly seen in the range of structural transformation of asphaltenes at ca. 40 ^{o}C (cf. Figure 5). Fairly straight segments, which allow evaluation of model parameters, are observed for the "Cold" and the "Hot" states of the samples – in the ranges < 35 ^{o}C and > 58 ^{o}C (these limiting temperatures are indicated by vertical dashed lines in Figure 9).

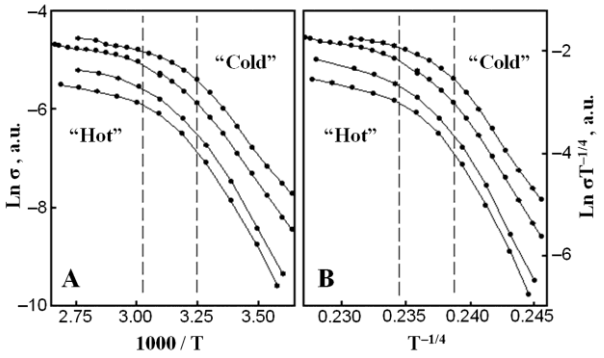

Figure 9. Analysis of conductivity parameters by applying two models of charge carrier excitation. A - Arrhenius-type model. B - "variable range hopping" (VRH) model.

Figure10 illustrates variations of evaluated model parameters E_a and T_0 in course of prolonged thermal treatment of asphaltene samples. Note, that in the Arrhenius-type model of Eq. (6) the pre-exponential factor σ_0 is presumed to possess only weak temperature dependence.

Hence, the observed increase/decrease of the measured conductivity σ in Figure 4 may be expected to result in the decrease/increase of the corresponding activation energy E_a. Figure 10A shows that the expected anti-correlation of σ and E_a is indeed observed almost in all cases. Note also, that in the as-deposited asphaltene film of sample #2, an activation energy in the "Hot" phase is virtually equal to a half of the higher energy gap ($E_a \approx E_{g1}/2$ – dashed line **a** in Figure 10A) suggesting a predominance of inter-band electron excitation. The loss of film homogeneity in course of thermal treatment results in a decrease of E_a towards the value of $E_b/2$ (dashed line **b**). Correspondingly, in a non-homogeneous powder sample #2 all E_a values are close $E_b/2$. In the powder sample #1, the lower energy gap E_{g2} appears to be more important. Here, an increase of homogeneity in sintered powder is accompanied by an increase of "Cold" E_a from the initial values of $E_{g2}/2$ (dashed line **c**) towards the value of $E_{g1}/2$. The dashed line **d** in Figure 10A indicates an additional energy parameter ($E_a \approx 0.25$ eV) being of apparent importance for conductivity in both samples. In case it is also related to some optical energy gap (absorption band), the respective gap/band energy, 0.5 eV, should correspond to IR wavelengths (ca. 2480 nm), well outside the range of our optical measurements. Literature analysis shows that that in IR spectra of asphaltenes there is a strong absorption band around 2440 nm, attributed to –C–H stretching and bending vibrations.[46] With respect to interrelation of conductivities and activation energies, the only "anomalous" case in Figure 10A is the "Cold" phase of film sample #2, where E_a exhibits direct correlation with changes of σ in Figure 4. As concluded below, such "anomaly" may be due to a failure of the Arrhenius-type model.

The behavior of VRH parameters in Figure 10B at first glance may appear similar to the behavior of activation energies. However, an additional Meyer–Neldel analysis reveals important

differences, related to the presence of VRH conductivity mechanisms in the asphaltene film (cf. Figure 11).

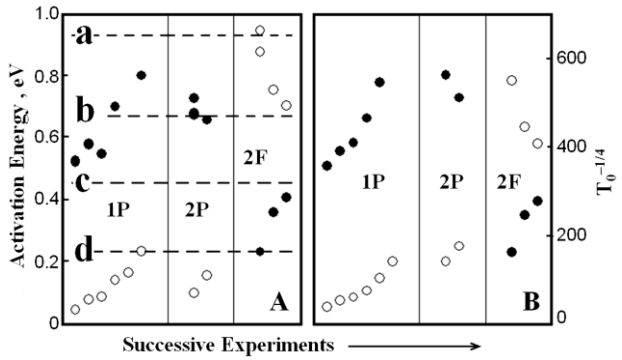

Figure 10. Effects of prolonged thermal treatment of asphaltene samples #1 and #2 in a powder state (**1P**,**2P**) and in a film state (**2F**) on parameters of two conductivity models. **A** – activation energies E_a in the Arrhenius-type model (dashed lines a, b and c indicate halves of optical energy gaps E_{1g}, E_b and E_{2g}). **B** – characteristic temperatures T_0 in the VRH model. Filled symbols – lower temperature "Cold" phase; open symbols – higher temperature "Hot" phase.

The above discussed data of Figure 10A appear to support the mechanisms of conduction via thermally activated electron excitations. In particular, in the as-deposited "Hot" asphaltene film, inter-band excitations clearly are of primary importance. However, according to the current theories of electron transport in non-crystalline materials,[44,45] the activation energies by themselves do not fully characterize the predominant conductivity mechanisms. The classical energy band scheme describing a crystalline material, changes in the amorphous case so that the valence and conduction bands stretch out and develop "tails" while a middle allowed band (compensated levels) also shows up near the center of the forbidden band gap. Carriers with energies within the tails and the central band are described by spatially localized states while for other energies the carriers are in extended (non-localized) states. Hence, there may be present three (superimposed) mechanisms of charge transport: (i) in the free-carrier mechanism, charge

carriers are thermally excited across comparatively large energy gaps into extended states; (ii) in the nearest-neighbor hopping mechanism, the carriers move between spatially close "shallow" localized states in the valence and conduction band tails; (iii) in the "variable-range hopping" (VRH) mechanism, conduction occurs by tunneling between "deep" energetically close localized traps in the middle band near the Fermi level.

For cases (i) and (ii), the temperature dependences of σ predicted by these models are Arrhenius-type, though when nearest-neighbor hopping is involved, the pre-exponential factor σ_0 in Eq. (6) no longer remains constant. For VRH conduction in case (iii), $\sigma(T)$ can be written as in Eq. (8). Important information on particular conductivity mechanisms may be obtained by considering the so-called Meyer–Neldel rule (MNR),[47,48] which has been widely employed for analysis of conductivity since its discovery in 1937.[48] The MNR was observed in both crystalline and amorphous solids, in powdered and liquid semiconductors, as well as for nearest-neighbor hopping conductivity. The only necessary condition seems to be the presence of a certain degree of disorder in the material.

For Arrhenius-type models, the MNR states that the pre-factor σ_0 in Eq. (6) depends on the activation energy:

$$\sigma_0 = \sigma_{00}\exp(E_a/E_{MN}) \qquad (9)$$

where σ_{00} s a true constant and E_{MN} is the Meyer-Neldel energy which is thought to be characteristic of conduction involving extended states in the energy bands and localized states in the band tails.[47] The values of E_{MN} may be easily extracted from the slopes of $\ln(\sigma_0)$ vs. E_a plots, which should be linear if the MNR is valid.

Although our experimental results in Figure 10A show that the one-to-one correspondence between sample treatment history and activation energy does not exist, conductivity prefactors

and activation energies follow the Meyer–Neldel rule, as evidenced by linear plots in Figure 11A. Note that multiple, seemingly unrelated, data points from Figure 10A now form linear trends with just two distinctly different slopes. In particular, all "Hot" data for two powder samples and for the film sample form a single NMR line with the slope characterized by E_{MN} = 33.8 meV. A virtually equal value of E_{MN} (33.2 meV) is inherent to a parallel NMR line for the "Cold" phase of samples in the powder state. In contrast, "Cold" data for the asphaltene film form a noticeably different straight line with much lower E_{MN} = 21.4 meV. The "anomalous" behavior of this data set suggests that the Arrhenious-type interpretation is not fully applicable for description of bulk conductivity mechanisms in "Cold" asphaltenes. This suggestions is also supported by the below discussed MNR analysis of VRH parameters (cf. Figure 11B).

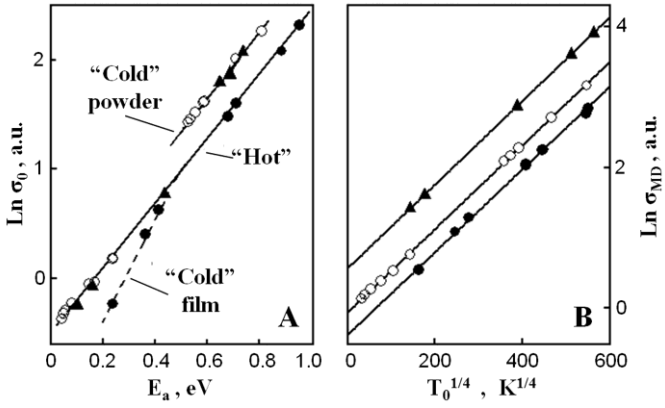

Figure 11. Application of the Meyer–Neldel analysis to asphaltene conductivity data in Figure 9. Open circles – sample #1, powder; filled triangles - sample #2, powder; filled circles – sample #2, film. A - Arrhenius-type model. B - VRH model.

The observed values of E_{MN} in asphaltenes may be further interpreted on the basis of recent theories. Though it has been repeatedly reminded that the Meyer–Neldel rule is an empirical one,[47,48] some plausible explanations have been proposed. E.g., some models predict that the origin for MNR lies in the distribution of trap states which appear at band tails due to disorder in a particular atomic/molecular structure.[49,50] Accordingly, E_{MN} is thought to give the

width of this distribution. Figure 11A shows the presence of NMR and the constancy of E_{MN} for asphaltene samples with different pre-treatment (#1 and #2), with different macrostructure (powder and film), in different structural phases ("Cold" and "Hot") and in different stages of thermal aging. This indicates that, in conditions of our experiments, distribution of band tail states is determined solely by the molecular nature of asphaltenes. On the other hand, occupation of these states apparently is affected by thermally-induced structural transformations. I.e., in "Cold" powders E_a values are compatible with nearest-neighbor hopping between localized states close to the band edges, while in "Hot" samples, smaller E_a may indicate involvement of occupied states further removed into the band tails.

Furthermore, some authors argued that the thermal energy $E_{MN} = kT_{MN}$ is not just a characteristic parameter of state distribution. It has been suggested that T_{MN} may be interpreted as a real physical temperature, namely a "glass transition" temperature.[51] In this model, a term "glass transition" was employed in a generalized sense, to describe various structural transformations resulting in a frustration of atomic/molecular thermal motion. It was further argued that a "glass transition" at $T = T_{MN}$ is the origin of the particular distribution of trap states. Information on the state of thermal disorder at the transition is "conserved" in the value of E_{MN} for sample properties at other temperatures. It must be emphasized, however, that at present this model is only a conjecture and there exists no conclusive experimental evidence in its favor. Nevertheless, evaluation of "transition temperatures" from the E_{MN} energies in Figure 11A results in apparently meaningful values of T_{MN}. Disregarding the "anomalous" case of "Cold" film, the values of E_{MN} = 33.2 and 33.8 meV correspond to T_{MN} = 112 and 119 ^{o}C, close to a "bulk" transition in asphaltenes observed just above 105 - 110 ^{o}C[28,29] (cf. discussion of Figures 5 and 6). The virtual coincidence of E_{MN} values for "Hot" and "Cold" data again suggests that phase

transition at ca. 40 ^{o}C is not truly reversible – at lower temperatures the "Hot" distribution of traps is retained.

In the VRH models, the analogue of Meyer-Neldel rule is a dependence of the pre-factor σ_{MD} in Eq. (8) on the "characteristic temperature" T_0.

$$\sigma_{MD} \sim \exp[(T_0/T_{VRH})^{1/4}] \qquad (10)$$

The value of Meyer-Neldel parameter $T_{VRH}^{1/4}$ may be extracted the slope of $\ln(\sigma_{MD})$ vs. $T_0^{1/4}$ plot. As above, the corresponding energy kT_{VRH} may be regarded as a measure of electron states distribution, involved in variable range hopping transport of charge carriers. Figure 11B shows that the overall behavior of our experimental data is better accounted for by VRH-type models, than by Arrhenius-type models. In particular, the MNR plots for VRH parameters from Figure 10B do not exhibit any "anomalies" and constitute three parallel straight lines with a common kT_{VRH} = 27.3 meV. As discussed below, the reason for a quantitative difference from E_{MN} = 33.2 - 33.8 meV may be that E_{MN} characterizes the distribution of states for "shallow" band-tale traps, while kT_{VRH} reflects the distribution of "deep" mid-gap traps. Note also, that in straight lines of Figure 11B the experimental data apparently are grouped according to macroscopic sample parameters (e.g., presence/absence of toluene-insolubles in samples #1 and #2, powder/film states of sample #2), while the data from Arrhenius-type analysis in Figure 11A are grouped with respect to microscopic "Hot" and "Cold" structural phases.

The specific features of the VRH model which provide its better suitability for our experiments may be the following. Firstly, as noted above, this model accounts not only for transport of free (collectivized) charge carriers and for unidirectional hopping of localized carriers between spatially neighboring traps, but also for a "random walk" hopping of carriers between traps close in energy, but of variable distances away from each other. Secondly,

Arrhenius-type models are known to account primarily for "shallow" traps in the band tails, while the VRH model accounts also for "deep" traps near the middle of the energy gap.[44,45] Thirdly, the use of Arrhenius-type approach and of the concept of activation energy seems to rely on an apparently common sense principle, that of "splittability of energy levels", which is not always working.[52] Well-splitted levels of localized traps may be expected to arise from dopants and impurities, while traps from structural disorder commonly possess a practically uniform (non-splitted) distribution of states.[44,52,53]

Summarizing, the results discussed in this section suggest a presence of both "bulk" and "surface" electron conductivity in asphaltenes, the latter being predominant in powder (dispersed) samples. In turn, three types of electron transport mechanisms, mentioned above, may be distinguished. "Bulk" mechanisms apparently are: a) a regular free carrier conduction involving delocalized extended states (energy bands) and predominant at higher studied temperatures (in the "Hot" phase) and b) "variable range" hopping between spatially unrelated "deep" traps with states in the middle of optical energy gap (predominant in the "Cold" phase). The principal "surface" conduction mechanism appears to be unidirectional electron transport by hopping between spatially neighboring "shallow" traps with states at band tails. Distributions of both "shallow" and "deep" trap states (characterized by values of E_{MN} and T_{VRH}) appear to be defined solely by the molecular nature of asphaltenes, while population of these states may be affected by the particular micro- and macro-structure of an individual sample.

The above conclusions may be of immediate relevance to studies of conductivity, dielectric properties and electrodeposition of asphaltene dispersions/suspensions in fluid media.[3-8,14,17]

E.g., observation of high surface conductivity of solid asphaltenes supports a hypothesis that the electrical conductivity in suspensions may originate from rapid charge exchange between

asphaltene colloidal particles.[54] Our results also show that colloidal particles comprised from asphaltene molecules with permanent dipole moments, in an external electric field may acquire additional induced dipole moments as a result of redistribution of intrinsic charge carriers. The importance of induced dipoles in asphaltene solutions/suspensions has been recognized[2,3,54] but, to our knowledge, has never been explicitly taken into account. Furthermore, effective hopping transport of electrons between asphaltene molecules may facilitate self-association of asphaltenes via charge transfer, as hypothesized more than a decade ago by Sheu et al.[55]

Measurements of Capacitance and Evaluation of the Dielectric Constant. Figure 12 shows typical capacitance *C* vs. temperature curves for powder asphaltene samples, measured in two heating/cooling cycles. In the above discussed "Cold" phase (below ca. 35 ^{o}C) capacitance did not exhibit any hysteresis and was temperature- and frequency-independent. Moreover, in contrast to conductivity measurement (cf. Figure 4), low-temperature constant *C* values were reproduced within ±1% in both powder samples at any stages of thermal aging. On the contrary, in the "Hot" structural phase of asphaltenes, capacitance always increased with increase of temperature and became dependent on frequency. As shown in Figure 12, at 120 Hz the rate of this increase was high and $C(T)$ curves exhibited a noticeable heating/cooling hysteresis, while measurements at 1000 Hz did not show any hysteresis and only a slight increase of *C* was observed at high temperatures.

The differences in the observed capacitance behavior in two structural phases of asphaltenes may have the same origin as the step-like change of dielectric loss-to-conductivity ratio in Figure 7. Namely, in the "Cold" phase the motion of dipolar moieties bound in asphaltene molecules is arrested as the principal inter-molecular interactions are via cross-linking of asphaltene side chains. In the "Hot" phase, π-interactions among aromatic moieties predominates

and the dipolar segments become more flexible. Enhancement of temperature-sensitive π-π bonding between condensed aromatic systems was observed to increase the measured capacitance,[56] while the increase of bound dipole flexibility in organic materials is frequently cited as a cause of the capacitance rise with temperature.[57,58] Capacitance increase was also interpreted as arising from an increase in a number of charge carriers and enhancement of the carrier hopping between localized traps (i.e., increase of conductivity) with increasing temperature.[58,59] Furthermore, the above capacitance-increasing effects were shown to be dependent on frequency - the capacitance was observed to attain high values in the quasi-static limit of low frequencies, decrease rapidly at frequencies above 100 Hz, and attain a constant value at higher frequency.[56-58]

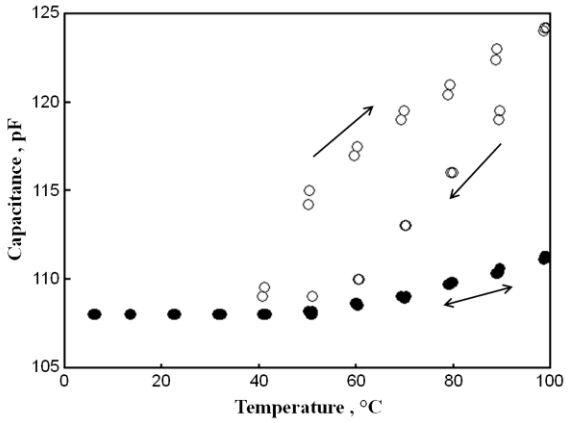

Figure 12. Temperature effects on capacitance, measured with asphaltene powders at different AC frequencies. Open circles – 120 Hz; filled circles – 1000 Hz.

The dielectric constant ε of asphaltenes was regarded as equivalent to the real part of the complex relative permittivity, ε' in the frequency-independent range (6 - 35 ^{o}C) of Figure 12. As follows from Eq. (2a), numerical evaluation of ε' from the measured C values requires a knowledge of two additional parameters, the lead capacitance C_L and the packing fraction ϕ of powder samples. The value of C_L was determined experimentally by calibration measurements

employing space-filling substances with well-known dielectric constants (air, toluene, *n*-decane and acetone). A possible range of the packing fraction was estimated on the basis of the following arguments. For a random arrangements of frictionless spheres the theoretical maximum value of the packing fraction is 0.64,[60,61] while the frictionless theoretical limits of non-spherical particles are $\phi = 0.575$ for cubes, 0.571 for cylinders and 0.547 for discs.[62] For gravity-packed natural powders in the presence of friction forces, commonly the values of ϕ below 0.5 are observed,[62,63] decreasing at smaller median/mean size of the particles.[62] E.g., for a grain size of 50 μm, packing fractions as small as 0.35 have been reported.[62] Mechanical compression may significantly increase the "natural" packing fractions (up to 0.70 - 0.74), but only if punch machines are employed at pressures as high as 150 - 200 MPa.[63] Asphaltene powders employed in our experiments contained irregular grains of ca. 11 μm median size and the samples were shaped in the presence of friction forces by very small compaction pressures below 0.1 MPa. Hence the data of the above discussed and of other relevant references suggest that in our studies the low and the high limits of the packing fraction are, approximately, $\phi = 0.4$ and $\phi = 0.5$.

Finally, we may conclude that the frequency-independent constant level of capacitance observed at 6 - 35 ^{o}C, corresponds to the following dielectric constant of asphaltenes: $\varepsilon = 4.3 \div 5.4$. These values, derived directly from studies of solid dry asphaltenes, are near the middle of ε range in Table 1, evaluated by various theoretical assumptions from earlier experiments with asphaltene solutions.[3,10-16]

Conclusions

While in multiple previous studies the term “electrical conductivity of asphaltenes” was misleadingly employed to characterize the movement of charged asphaltene colloids within crude oils and solvents, the subject of our experiments was electrical conductivity via the transport of charge carriers within solid asphaltenes themselves.

All studied samples show a conductivity increase at higher temperatures, typical for organic semiconductors. Furthermore, we conclude that in solid asphaltenes surface conductivity is always predominant over the bulk one. To get insight into particular transport mechanisms of charge carriers, the results of conductivity measurements are supplemented by comparison of UV-vis-NIR absorption spectra for solid asphaltenes and for their solution in toluene. The obtained experimental data are analyzed within the formalisms of Arrhenius-type and Mott-Davis conductivity models by application of the Meyer–Neldel rule. This analysis suggests that bulk conductivity at higher temperatures occurs via thermal excitation of electrons between extended states (energy bands), while at lower temperatures the main mechanism is “variable range hopping” of electrons between spatially unrelated, but close in energy, deep localized traps. The main transport mechanism of charge carriers at asphaltene surfaces appears to be unidirectional “nearest neighbor” electron hopping between spatially close shallow localized traps.

The dielectric constant of solid asphaltenes below 35 - 40 ^{o}C was found to be both frequency and temperature independent and was evaluated as $\varepsilon = 4.3 \div 5.4$. These values, derived directly from studies of solid asphaltenes, are near the middle of the range, evaluated by various theoretical assumptions from earlier experiments with asphaltene solutions.

The temperature dependencies of measured parameters reveal the presence of a structural phase transition in asphaltenes. Taking into account the relationship of dielectric loss to

conductivity, this transition may be ascribed to changes in the predominant type of intermolecular bonding. The low-temperature “Cold” phase appears to be controlled by interactions between polar side chains of asphaltene molecules, while in the high-temperature “Hot” phase π-π interaction involving flat polyaromatic structures in asphaltenes apparently become more important. Our results indicate that at solid surfaces this phase transition occurs at absolute temperatures about 20% lower than in the solid bulk.

The obtained results may be of immediate relevance to studies of conductivity, dielectric properties and electrodeposition of asphaltene dispersions/suspensions in crude oils and solvents. E.g., these results indicate the importance of induced dipole moments in asphaltene colloids and also show that the electrical conductivity in suspensions may originate from rapid charge exchange between asphaltene colloidal particles. Furthermore, effective hopping transport of electrons between asphaltene molecules may facilitate self-association of asphaltenes in crude oils.

References

(1) Chilingarian, G. V.; Yen, T. F. Introduction to asphaltenes and asphalts. In *Asphaltenes and Asphalts, 2*; Yen, T. F., Chilingarian, G.V., Eds.; Elsevier: Amsterdam, 2000. p.1-6.

(2) Sheu, E. Y.; Acevedo, S. A dielectric relaxation study of precipitation and curing of Furrial crude oil. *Fuel* **2006**, *85*, 1953-1959.

(3) Rejon, L.; Manero, O.; Lira-Galeana, C. Rheological, dielectric and structural characterization of asphaltene suspensions under DC electric fields. *Fuel* **2004**, *83*, 471-476.

(4) L. Goual, L. Impedance spectroscopy of petroleum fluids at low frequency**.** *Energy Fuels* **2009,** *23,* 2090-2094.

(5) Lichaa, P.M.; Herrera, L. Electrical and other effects related to the formation and prevention of asphaltenes deposition. *Soc. Pet. Eng. J.* **1975**, paper #5304.

(6) Fotland, P.; Anfindsen, H. Conductivity of asphaltenes. In *Structure and dynamics of asphaltenes*; Mullins, O. C.; Sheu, E. Y., Eds.; Plenum Press: New York, 1998. p.247-266.

(7) Hasnaoui, N.; Achard, C.; Rogalski, M.; Behar, E. Study of asphaltene solutions by electrical conductivity measurements. *Rev. Inst. Fr. Pet*. **1998**, *53*(1), 41-50.

(8) Fotland, P.; Anfindsen, H.; Fadnes, F. H. Detection of asphaltene precipitation and amounts precipitated by measurement of electrical conductivity. *Fluid Phase Equilib.* **1993**, *82*, 157-164.

(9) Sheu, E. Y.; Storm, D. A.; Tar, M. M. D. Asphaltenes in polar solvents. *J. Non-Cryst. Solids* **1991**, *131-133*, 341–347.

(10) Akhmetova, R. S.; Glozman, E. P. Asphalt quality as influenced by nature of asphaltenes. *Chem. Technol. Fuels Oils* **1974**, *10*(7), 540-542.

(11) Pedersen C. *Asphaltene characterization: permittivity measurements and modeling*. Ph.D. Thesis. Technical University: Lyngby, Denmark, 2000.

(12) Tao, R.; Xu, X. Reducing the viscosity of crude oil by pulsed electric or magnetic field. *Energy Fuels* **2006,** *20,* 2046-2051.

(13) Maruska, H. P.; Rao, B. M. L. The role of polar species in the aggregation of asphaltenes. *Fuel Sci. Technol. Int.* **1987**, *5*(2), 119-168.

(14) Taylor, S. E. The electrodeposition of asphaltenes and implications for asphaltene structure and stability in crude and residual oils. *Fuel* **1998**, *77*(8), 821-828.

(15) Oudin, J. L. Analyse geochimique de la matiere organique extraite des roches sedimentaires I. Composes extractibles au chloroforme. *Rev. Ins. Fr. Pet.* **1970**, *25*(1), 4.

(16) Goual, L.; Firoozabadi, A. Measuring asphaltenes and resins, and dipole moment in petroleum fluids. *AIChE J.* **2002**, *48*(11), 2646–2663.

(17) Vralstad, H. Spets, Ø.; Lesaint, C.; Lundgaard, L.; Sjoblom, J. Dielectric properties of crude oil components. *Energy Fuels*, **2009**, *23*(11), 5596–5602.

(18) Garrett, C. G. B. Organic Semiconductors. *Radiation Res. Suppl*. **1960**, *2*, 340-348.

(19) Forster, E. O. On the activation energy for conductance in aromatic hydrocarbons. *Electrochim. Acta* **1964**, *9*(10), 1319-1327.

(20) Masson, J. -F.; Polomark, G. M.; Collins, P. Time-dependent microstructure of bitumen and its fractions by modulated differential scanning calorimetry, *Energy Fuels*, **2002**, *16*(2), 470–476.

(21) Maham, Y.; Chodakowski, M. G.; Zhang, X.; Shaw, J. M. Asphaltene phase behavior: prediction at a crossroads. *Fluid Phase Equilib.* **2005,** *227*(2), 177-182.

(22) Rodriguez-Abreu, C.; Delgado-Linares, J. G.; Bullon, J. Properties of Venezuelan asphaltenes in the bulk and dispersed state. *J. Oleo Sci*. **2006**, *55*(11), 563-571.

(23) Fulem, M.; Becerra, M.; Hasan, A.; Zhao, B.; Shaw, J. M. Phase behavior of Maya crude oil based on calorimetry and rheometry. *Fluid Phase Equilib.* **2008**, *272*(1-2), 32-41.

(24) Tran, K. Q. *Reversing and non-reversing phase transitions in Athabasca bitumen asphaltenes*. MSc. Thesis. University of Alberta: Edmonton, Canada. 2009.

(25) Ekulu, G.; Nicolas, C.; Achard, C.; Rogalski, M. Characterization of aggregation processes in crude oils using differential scanning calorimetry. *Energy Fuels* **2005**, *19*(4), 1297-1302.

(26) Puig, C. C.; Meijer, H. E. H.; Michels, M. A. J.; Segeren, L. H. G. J.; Vancso, G. J. (2004). Characterization of glass transition temperature and surface energy of bituminous binders by inverse gas chromatography. *Energy Fuels,* **2004**, *18*(1), 63–67

(27) Roux, J.-N.; Broseta, D.; Deme, B. SANS study of asphaltene aggregation: Concentration and solvent quality effects. *Langmuir* **2001**, *17*(16), 5085–5092.

(28) Evdokimov, I. N.; Eliseev, N. Yu. Thermally responsive properties of asphaltene dispersions. *Energy Fuels* **2006**, *20*(2), 682–687.

(29) Evdokimov, I. N.; Eliseev, N.Y. Electrophysical properties of liquid hydrocarbon media. *Chem. Technol. Fuels Oils* **2001**, *37*(1), 39–43.

(30) Verkerk, M. J.; Winnubst, A. J. A.; Burggraaf, A. J. Effect of impurities on sintering and conductivity of yttria-stabilized zirconia. *J. Mater. Sci*. **1982**, *17*(11), 3113-3122.

(31) Gittings, J. P.; Bowen, C. R.; Dent, A. C. E.; Turner, I. G.; Baxter, F.R.; Chaudhuri, J.B. Electrical characterization of hydroxyapatite-based bioceramics. *Acta Biomater.* **2009**, *5*, 743–754.

(32) Busch, B. W.; Gustafsson, T. Temperature dependent structure of clean Ag(110) studied by medium energy ion scattering. *Surf. Sci*. **1998**, *407*(1-3), 7–15.

(33) Yang, X.; Kilpatrick, P. Asphaltenes and waxes do not interact synergistically and coprecipitate in solid organic deposits. *Energy Fuels* **2005,** *19,* 1360-1375.

(34) Dubey, G.; Lopinski, G. P.; Rosei, F. Influence of physisorbed water on the conductivity of hydrogen terminated silicon-on-insulator surfaces. *Appl. Phys. Lett.* **2007**, *91*, 232111.

(35) Garcia-Belmonte, G; Kytin, V.; Dittrich, T.; Bisquert, J. Effect of humidity on the ac conductivity of nanoporous TiO_2. *J. Appl. Phys.* **2003**, *94*(8), 5261-5264.

(36) Nagai, M.; Nishino, T. Surface conduction of porous hydroxyapatite ceramics at elevated-temperatures. *Solid State Ionics* **1988**, *28–30*, 1456–1461.

(37) Tsutsui, T.; Fukuta, Y.; Hara, T.; Saito, S. Electronic conduction in poly(*p*-phenylene-1,3,4-oxadiazole) films. *Polym. J.* **1987**, *19*(6), 719-725.

(38) Anthopoulos, T. D.; Shafai, T. S. Alternating current conduction properties of thermally evaporated a-nickel phthalocyanine thin films: Effects of oxygen doping and thermal annealing. *J. Appl. Phys*. **2003**, *94*(4), 2426-2433.

(39) Jones, W. *Organic molecular solids. Properties and applications*. CRC Press: Boca Raton, 1997. – 448 p.

(40) Van De Craatz, A. M. *Charge transport in self-assembling discotic liquid crystalline materials*. Delft University Press: Delft, Netherlands, 2000. - 187 p.

(41) Adachi, S. *Optical properties of crystalline and amorphous semiconductors. Materials and fundamental principles*. Kluwer Academic Publishers: New York, 1999. - 280 p.

(42) Inokuchi, H. The electrical conductivity of the condensed polynuclear aromatic compounds. *Bull. Chem. Soc. Japan* **1951**, *24*(5), 222-226.

(43) Northrop, D. C.; Simpson, O. Electronic properties of aromatic hydrocarbons. I. Electrical conductivity. *Proc. Royal Soc. A* **1956**, *234*(1196),124-135.

(44) Mott, N. F.; Davis, E. A. *Electronic processes in non-crystalline materials, 2nd Ed*. Oxford University Press: Oxford, UK, 1979.

(45) Nagels, P. Electronic transport in amorphous semiconductors. In *Amorphous semiconductors*, Brodsky, M.H., editor. Springer-Verlag: Berlin, 1979. p.113-158.

(46) Peinder, P. de; Petrauskas, D. D.; Singelenberg, F. A. J.; Salvatori, F.; Visser, T.; Soulimani, F.; Weckhuysen, B. M. Prediction of long and short residue properties of crude oils from their infrared and near-infrared spectra. *Appl. Spectrosc.* **2008**, *62*(4), 414-422.

(47) Fisher, D. J. *The Meyer–Neldel rule*. Scitec Publications, Ltd: Zürich, 2002. - 372 p.

(48) Meyer, W.; Neldel, H. A. A relation between the energy constant ε and the quantity constant a in the conductivity-temperature formula for oxide. *Zeitschrift fuer Technische Physik* **1937**, *18*, 588-593.

(49) Meijer, E.J.; Matters, M.; Herwig, P.T.; de Leeuw, D.M.; Klapwijk, T.M. The Meyer-Neldel rule in organic thin-film transistors. *Appl. Phys. Lett*. **2000**, *76*(23), 3433-3435.

(50) Li, L.; Meller, G.; Kosina, H. Influence of traps on charge transport in organic semiconductors. *Solid-State Electronics* **2007**, *51*(3), 445-448.

(51) Dyre, J. C. A phenomenological model for the Meyer-Neldel rule. *J. Phys. C: Solid State Phys.* **1986**, *19*, 5655-5664.

(52) Ongaro, R.; Pillonnet, A. Failure of Arrhenius plots for investigation of localized levels. *Revue Phys. Appl*. **1990**, *25*, 209-227.

(53) Shklovskii, B. I.; Efros, A. L. *Electronic properties of disordered semiconductors.* Springer: Berlin, 1984.

(54) Sheu, E. Y.; Storm, D. A.; Shields, M. B. Dielectric response of asphaltenes in solvent. *Energy Fuels* **1994**, *8*, 552–556.

(55) Sheu, E. Y.; De Tar, M. M.; Storm, D.A. Dielectric properties of asphaltene solutions. *Fuel* **1994,** *73*(1), 45-50.

(56) Jeong, H.-K.; Jin, M. H.; An, K. H.; Lee, Y. H. Structural stability and variable dielectric constant in poly sodium 4-styrensulfonate intercalated graphite oxide. *J. Phys. Chem. C* **2009,** *113,* 13060–13064.

(57) Abd El Wahed, M. G.; Bayoumi, H. A.; Mohammed, M. I. Physical properties of some acetylbenzaldehydehydrazone metal complexes. *Bull. Korean Chem. Soc.* **2003**, *24*(9): 1313-1318.

(58) Kalugusalam, P.; Ganesan, Dr. S. Dielectric and ac conduction studies of lead phthalocyanine thin film. *Chalcogenide Lett.* **2009**, *6*(9), 469-476.

(59) Su, J. S.; Chen, Y. F.; Chiu, K. C. Dielectric properties of C60 films in the high-temperature region. *Appl. Phys. Lett*. **1999**, *75*(11), 1607-1609.

(60) Clusel, M; Corwin, E. I.; Siemens, A. O. N.; Brujic, J. A "granocentric" model for random packing of jammed emulsions. *Nature* **2009**, *460*, 611-616.

(61) Kansal, A. R.; Torquato, S.; Stillinger, F. H. Computer generation of dense polydisperse sphere packings. *J. Chem. Phys*. **2003**, *117*(18), 8212-8218.

(62) Glover, P. W. J. *Formation Evaluation*. Université Laval: Québec, Canada, 2002. p. 43-53.

(63) Rahmouni, M.; Lenaerts, V.; Massuelle, D.; Doelker, E.; Leroux, J.-C. Influence of physical parameters and lubricants on the compaction properties of granulated and non-granulated cross-linked high amylose starch. *Chem. Pharm. Bull.* **2002**, *50*(9), 1155-1162.